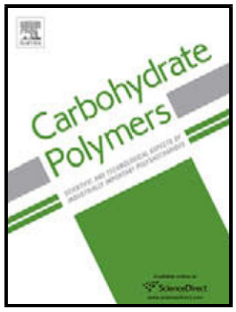

Title: Effects of amine loading on the properties of cellulose nanofibrils aerogel and its CO_2 capturing performance

Authors: Yu Wu, Yang Zhang, Nanqing Chen, Sheng Dai, Hua Jiang, Siqun Wang

PII: S0144-8617(18)30397-7
DOI: https://doi.org/10.1016/j.carbpol.2018.04.017
Reference: CARP 13471

To appear in:

Received date: 13-2-2018
Revised date: 27-3-2018
Accepted date: 3-4-2018

Please cite this article as: Wu, Yu., Zhang, Yang., Chen, Nanqing., Dai, Sheng., Jiang, Hua., & Wang, Siqun., Effects of amine loading on the properties of cellulose nanofibrils aerogel and its CO2 capturing performance.*Carbohydrate Polymers* https://doi.org/10.1016/j.carbpol.2018.04.017

Effects of amine loading on the properties of cellulose nanofibrils aerogel and its CO_2 capturing performance

Yu Wu, [a,c] Yang Zhang, [b] Nanqing Chen, [d] Sheng Dai, [d] Hua Jiang, [a] Siqun Wang, [c]

[a]College of Chemical Engineering, Nanjing Forestry University, Nanjing 210037, China

[b]College of Material Science and Engineering, Nanjing Forestry University, Nanjing 210037, China

[c]Center for Renewable Carbon, University of Tennessee, Knoxville, TN 37996, USA

[d]Department of Chemistry, University of Tennessee, Knoxville, TN 37996, USA

[*]Corresponding authors: jianghua@njfu.com.cn, College of Chemical Engineering, Nanjing Forestry University, Nanjing 210037, China; swang@utk.edu, Center for Renewable Carbon, University of Tennessee, Knoxville 37996, USA

Highlights

- Amine-based hybrid aerogel adsorbents were successfully prepared via
- one-step chemical react without previous gelation.
- The effects of amine loading on the properties of CNF were investigated.
- The regeneration process of the aerogel sorbents was simply heating.

Abstract

In this work, cellulose nanofibrils (CNFs) were used to develop novel amine-based aerogels that can be applied as adsorbents for CO_2. Elemental analysis indicated that

there was an increase in the C and N content when the concentration of aminosilane was higher. Moreover, Fourier transform infrared spectroscopy confirmed that the aminosilane had been grafted on the CNF. Thermal analysis and X-ray diffraction revealed that the thermal stability of the aerogel decreased after the modification, and the crystallinity decreased. However, the higher amine loading led to a rougher CNF surface and a larger average pore size, which favored the CO_2 capture. Furthermore, CNF grafted with aminosilane displayed a high CO_2 adsorption capacity (1.91 mmol/g 25 ° C，1 bar) and an easy regeneration process by heating at 80 ° C. Therefore, the prepared polymer aerogels might have a highly potential use in the capture of CO_2.

Keywords: cellulose nanofibril, aminesilane, sorbent, CO_2 capture

1. Introduction

Nowadays, with the increasing amount of energy consumption, the growing level of CO_2 released into the atmosphere has resulted in severe environmental problems. In particular, global warming has generated widespread environmental concerns about the continued use of carbon-based fuels (Sumida et al., 2012). Over the past decades, numerous efforts have been devoted to mitigating this problem by capturing CO_2 from major source points such as coal, petroleum, and gas-fired power plants (Aaron & Tsouris, 2005; Haszeldine, 2009; Jones, 2011). A wide range of approaches, including physical and chemical adsorption, as well as membrane separation processes, has been reported in the literature (Aroonwilas & Veawab, 2007; Yu, Curcic, Gabriel & Tsang,

2008). Of all approaches, chemical adsorption based on aminosilane is currently one of the most effective one for the capture and separation of CO_2 (Jiao, Cao, Xia & Zhao, 2016).

Previous synthetic routes to amine-based adsorbent materials employed mainly inorganic materials as support (Choi, Drese & Jones, 2009). However, the development of bio-based sorbents with excellent CO_2 adsorption properties is a promising alternatives to inorganic materials. Several sustainable and biomass-derived products have been used as precursors for the production of carbon sorbents, including lignin (Sangchoom & Mokaya, 2015), biomass (sawdust) (Sevilla & Fuertes, 2011), alginate (Primo, Forneli, Corma & Garcia, 2012) and cellulose (Cheng, Wang, Rials & Lee, 2007; Gebald, Wurzbacher, Tingaut, Zimmermann & Steinfeld, 2011). In an attempt to promote the use of natural renewable resources for the development of porous carbon materials, cellulose nanofibrils (CNFs) aerogels as solid support has attracted intensive attention by many researchers due to its renewable and environmentally friendly nature (Meng, Young, Liu, Contescu, Huang & Wang, 2015). Aerogels are nanoporous materials with a three-dimensional network, low density, high specific surface area and small pore size, which are beneficial for capturing gas (Linsha, Mohamed & Ananthakumar, 2015; Zu, Shen, Wang, Zou, Lian & Zhang, 2015). Furthermore, the abundance of hydroxyl groups on CNF can allow it to be grafted with a myriad of aminesilane, which could improve the CO_2 adsorption capacity (Habibi, Lucia & Rojas, 2010). For example, Pacheco et al. prepared an aminosilane-functionalized cellulosic

polymer sorbent with enhanced CO_2 sorption capacity to capture CO_2 from postcombustion gas stream (Pacheco, Johnson & Koros, 2012). In addition, Rownaghi et al. developed aminosilane-grafted hollow fiber composites for CO_2 capture, which exhibit a relatively high CO_2 capture capacity at atmospheric pressure and under dry conditions (Rownaghi et al., 2016). Brennan et al. demonstrated the aminosilane-grafted hollow fiber sorbents with a higher amine loading and a higher CO_2 capture capacity (Brennan, Thakkar, Li, Rownaghi, Koros & Rezaei, 2017). These studies indicated that nanocellulose aerogels modified by amine could be applied as high-performance CO_2 adsorbents.

Among the various agents that could be employed to modify CNF are coupling agents such as aminosilane reagents (Kalia, Boufi, Celli & Kango, 2014). However, silane reagents with three alkoxy groups are prone to hydrolysis and self-polymerization on the CNF surface, which is unfavorable for CO_2 capture as the inner pore structure is likely to be blocked (Wu, Cao, Jiang & Zhang, 2017). Therefore, aminosilanes with two alkoxy groups have been employed in order to avoid undesired blocking of functional amine sites. Moreover, the effects of aminesilane modification on the aerogel properties and the structure of the aerogel fabricated from the amined-modified CNFs are important but little literature was reported.

Recently published studies focused on the modified aerogels obtained via solvents for gelation (Gavillon & Budtova, 2008; Nguyen, Feng, Ng, Wong, Tan & Duong, 2014). However, in this study, amine aerogel was prepared only by one-step chemical react

with no previous gelation process. The primary objective of this study was to investigate the effect of aminesilane modification on the properties of resultant CNF aerogels, as well as the CO_2 capture performance of the aerogel. The structural changes of aerogels were characterized using Fourier transform infrared spectroscopy (FTIR) and X-ray diffraction (XRD). The thermal properties of the aerogels were studied using thermogravimertic analysis (TGA) and the elemental changes were determined by energy-dispersive X-ray (EDX) spectra after modification.

2. Experimental

2.1. Materials

CNF (3 wt.%, 3-100 nm in width and up to several micron in length) was purchased from the University of Maine, Process Development Centre. N-(2-aminoethyl)-3-aminopropylmethyldimethoxysilane (APS, 97% purity) and tertiary butanol (TBA, 99.7% purity) were obtained from Fisher Scientific (USA).

2.2 Preparation of CNF grafted with APS

CNF (20g, 3 wt.%) and TBA (80g, 97 wt.%) were placed into a 500 mL round-bottom flask under magnetic stirring. The pH of the mixture was adjusted to 3 by adding a few drops of acetic acid to avoid self-polymerization as soon as possible (Fig. 1). Because according to previous report (She, Zhang, Song, Lang & Pu, 2013), it is beneficial to form more reactive silanol groups and the retardation of their condensation rate under

acidic conditions when the aminesilanes hydrolysis. This, in turn, makes them accessible to react with the hydroxy groups of the cellulose, or to condensate over the fiber surface. After the temperature of the mixture was raised to 90 ° C, APS (2, 4, 6, and 8 wt.%) was added and the solution was refluxed for 3 h at 90 ° C. Then, the heat was turned off and the solution was centrifuged / washed with TBA solution twice to remove the excess APS. Then some of the sediment was taken out to test the solid content, the others was diluted with TBA to 3 wt. % for all samples. Lastly, the suspension were poured in a copper cylinder that was then immersed in liquid N_2 and the frozen sample was dried with a freeze dryer (LABCONCO Co.). The CNF samples treated with different amounts of APS (2, 4, 6, and 8 wt.%), were denoted as CNF+APS-2%, CNF+APS-4%, CNF+APS-6%, and CNF+APS-8%, respectively. In addition, the synthesis route of polymer aerogel and its adsorption mechanism were schematically displayed in Fig. 1:

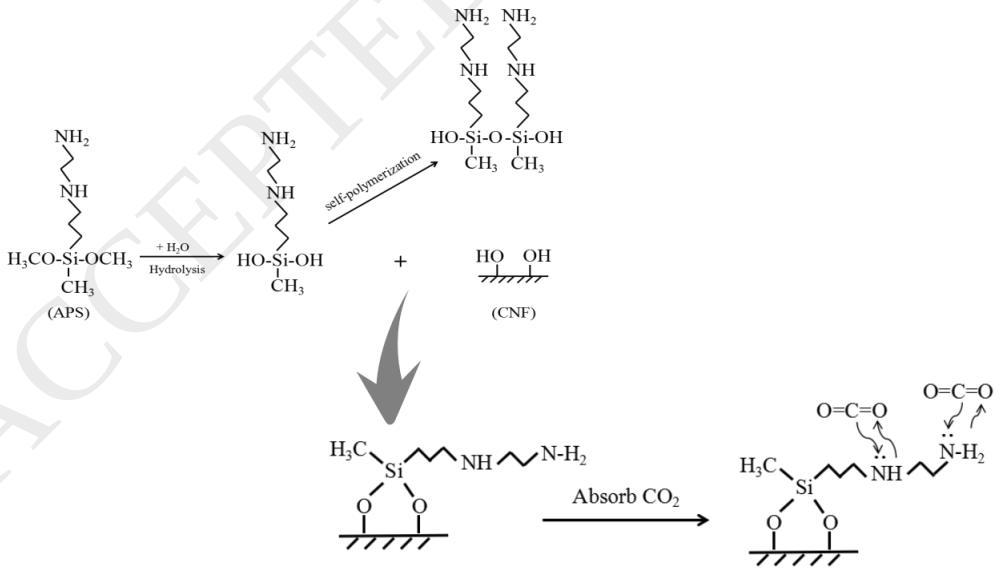

Fig 1. Schematic description of synthesis route of polymer aerogel and its adsorption

mechanism

2.3. Characterizations

2.3.1. Fourier transform infrared (FTIR) spectra. The infrared absorption spectra of the samples were recorded using a Perkin Elmer FTIR-ATR spectrometer (Spectrum One, Perkin Elmer, USA). All samples were reserved in the dryer before the measurements. The spectra were recorded in the range from 4000 to 500 cm^{-1}.

2.3.2. Energy-Dispersive X-ray (EDX) Spectra. Elemental analysis was carried out using EVO-MA15 (XFlash 6130, Bruker, Germany). The content of the relative elements of all samples was determined by EDX spectrometry. The measurement conditions were the same as those used for SEM characterization.

2.3.3 X-ray diffraction (XRD)

The XRD pattern of each sample was evaluated using an X-ray diffractometer (Rigaku, Japan) with Ni-filtered Cu Kα radiation (λ= 0.1541 nm), which was operated at 40 kV and 40 mA. The scattered radiation was detected in the range of 2θ = 5-40° at a scan rate of 2°/min. The crystallinity index (CrI) was calculated for each sample by using the following equation which was introduced by Segal et al.(L. Segal, 1959):

$$CrI(\%) = \frac{I_{002} - I_{am}}{I_{002}} \times 100\% \qquad (1)$$

where I_{002} is the maximum intensity of the crystallinity of the diffraction peak, and I_{am} is the intensity scattered by the amorphous part of the sample.

The crystal size and d-spacing of the samples were calculated from the Scherrer's and Bragg's equations (Garvey, Parker & Simon, 2005; Lee, Quero, Blaker, Hill, Eichhorn & Bismarck, 2011), respectively:

$$L_{(hkl)} = \frac{k\lambda}{\beta \cos\theta} \qquad (2)$$

$$d_{(hkl)} = \frac{\lambda}{2\sin\theta} \qquad (3)$$

where (hkl) is the lattice plane, L(hkl) is the crystal size, k is the Scherrer's constant (0.91), λ is the X-ray wavelength (0.154 nm), β is the full width half maximum of the measured hkl reflection, 2θ is the corresponding Bragg's angle, and d(hkl) is the d-spacing of the lattice plane (hkl).

2.3.4. Thermogravimetric Analysis (TGA). TGA was carried out on Pyris 1 TGA (Perkin Elmer, USA). The temperature of all samples were scanned over a range from 30 to 800 °C at a heating rate of 10 °C/min. Nitrogen was given at a flow rate of 10 mL/min to avoid sample oxidation.

2.3.5. Scanning electron microscopy (SEM) micrograph. The morphologies and structures of the samples were investigated using the Quanta200 scanning electron microscope (FEI, USA) under vacuum at an operating voltage of 10 kV. Before the examination, a fine layer of gold was sprayed on the samples using an ion sputter coater with a low deposition rate.

2.3.6. N_2/CO_2 sorption isotherms. CO_2 adsorption isotherms were obtained at 25 °C

on an Autosorb 1C instrument (Quantachrome Instruments, USA). Prior to the adsorption analysis, the sample was degassed at 80 °C for 5 h.

3. Results and discussion

3.1 FTIR Characterization

FTIR spectroscopy is an appropriate technique to monitor the variations in the chemical composition of the samples. It has been extensively applied for structural analysis of materials before and after chemical treatments. The effects of introducing APS on the CNF examined with an FTIR spectroscopy are presented in Fig. 2(i). It was shown that the spectra of all samples were similar. The band observed at 3340 cm^{-1} was assigned to an O-H vibration resulted from the hydrogen bonds in cellulose I (Hosseinaei, Wang, Enayati & Rials, 2012; Hosseinaei, Wang, Taylor & Kim, 2012). The bands at 2928 and 2875 cm^{-1} were associated with C-H stretching vibration (Anuj Kumar, 2014; Knoefel, Martin, Hornebecq & Llewellyn, 2009a), and the band at 897 cm^{-1} was associated with the ring vibration of the C_1-H deformation (Lu, Askeland & Drzal, 2008).

However, new peaks appeared after the CNF was treated using APS. The appearance of the band at 1255 cm^{-1}, attributed to a C-O-Si stretching vibration (Wu, Cao, Jiang & Zhang, 2017), proved that APS was successfully grafted on the CNF surface. And the band at 1460 cm^{-1} was assigned to C-H_2 bending of the silane propyl

chain (Knoefel, Martin, Hornebecq & Llewellyn, 2009b). Moreover, the band at 796 cm^{-1} was related to the stretching vibration of the Si-C or Si-O bonds (Popescu, Singurel, Popescu, Vasile, Argyropoulos & Willfor, 2009; Zhang, Sebe, Rentsch, Zimmermann & Tingaut, 2014). In addition, the intensity of these new bands became

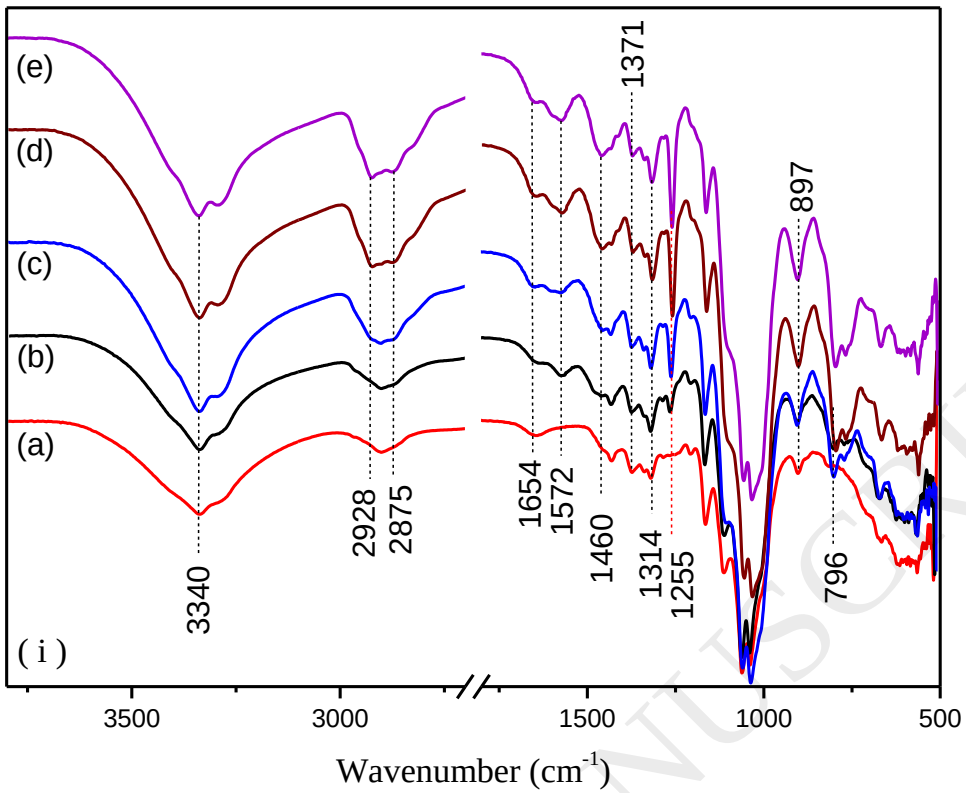

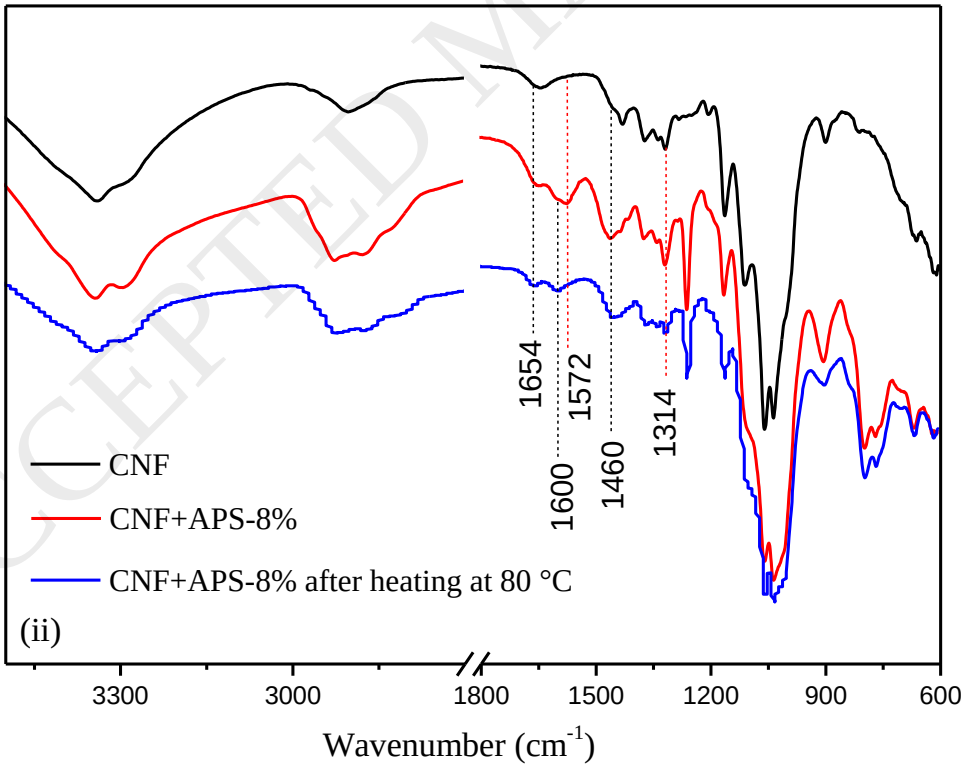

Fig. 2 (i) FTIR spectra of (a) CNF, (b) CNF+APS-2%, (c) CNF+APS-4%, (d)

CNF+APS-6%, and (e) CNF+APS-8%, (ii) FTIR spectra of CNF, CNF+APS-8%, and CNF+APS-8% after heating at 80° C

stronger with the increasing amount of added APS, which indicated that higher APS concentration favored the modification. However, these bands were similar in their intensity after APS concentration of 6 wt. %. This phenomenon might be due to the saturation of the hydroxyl groups on the CNF surface with APS.

Moreover, the band at 1572 cm^{-1} was ascribed to an (N)COO- asymmetric stretching (Bacsik, Atluri, Garcia-Bennett & Hedin, 2010), and the one at 1314 cm^{-1} was associated with the symmetric stretching of (N)COO- (Danon, Stair & Weitz, 2011). A plausible explanation of these results might be that the APS grafted on the CNF captured CO_2 from the air. This CO_2 then reacted with primary and secondary amines to form carbamic acid, carbamate, and bicarbonate species (Robinson, McCluskey & Attalla, 2011; Versteeg, Van Dijck & Van Swaaij, 1996). To prove this possibility, a spectrum of CNF+APS-8% after heating at 80 ° C (higher temperature favored the CO_2 desorption) was showed in Fig. 2(ii). As can be seen, both peaks at 1314 and 1572 cm^{-1} of CNF+APS-8% become very weak or even disappeared after heating at 80 °C. This observation supported the possible explanation of the phenomenon mentioned previously, and implied that the CO_2 captured by APS on the CNF surface could be desorbed by heating.

3.2 Elemental analysis

Table 1 Relative element content of all samples

Samples	Elemental analysis（atom%）		
	C	O	N
CNF	55.3	44.7	0
CNF+APS-2%	54.8	39.3	4.1
CNF+APS-4%	55.4	35.7	6.5
CNF+APS-6%	55.9	32.1	8.1
CNF+APS-8%	56.1	31.2	8.3

EDX spectroscopy was employed to investigate the relative element change of CNF after modification with APS (Table 1). As can be seen from Table 1, with the increase in added amount of APS, the content of carbon increased from 55.3 to 56.1%. In addition, the nitrogen content increased from 0 to 8.3 while the oxygen content decreased from 44.7 to 31.2%. The disagreement of the changes in oxygen and carbon contents was mainly due to the introduction of APS that contained 8 carbon and only 2 oxygen atoms. This observation was in agreement with one reported by Hokkanen et al. (Hokkanen, Repo, Suopajarvi, Liimatainen, Niinimaa & Sillanpaa, 2014). Moreover, the nitrogen contents in the samples were nearly equal, which might be due to the hydroxyl group saturation, as observed previously in the FTIR analysis. This result further suggested that APS had successfully been grafted on the surface of CNFs.

3.3 Thermogravimetric analysis

Fig. 3(i) and (ii) showed the TGA and differential thermogravimetric (DTG) curves of samples before and after the modification. The initial weight loss of the modified samples observed at about 60 °C could be attributed to the desorption of CO_2 captured from air, which was in agreement with the analysis of FTIR in Fig. 2 (ii) and part of free water on the sample. The second weight loss, observed at about 100°C in all samples, was ascribed to the removal bonded water (Wu, Cao, Jiang & Zhang, 2017). As shown in the TG curves, the thermal decomposition of CNF started at about 265 °C, followed by a drastic weight loss from 320 to 430 °C, and then a slight decrease. Meanwhile, the weight loss of the modified samples occurred at a broader range from 247 to 587 °C. Notably, when the amount of added APS was over 2 wt.%, two decomposition peaks were obviously observed in the spectra of the modified samples, starting from about 350 °C and 443 °C (Fig. 3ii). What's more, with increasing the concentration of APS, the residues of polymer aerogels increased. These results were mainly because the introduction of APS enhanced the interaction between CNF and aminosilane, and produced new substance that is difficult to degrade during the heating process and increased the residues (Zhai, Zheng, Cai, Xia & Gong, 2016). Therefore, the thermal stability of CNF after modification has a slight decrease.

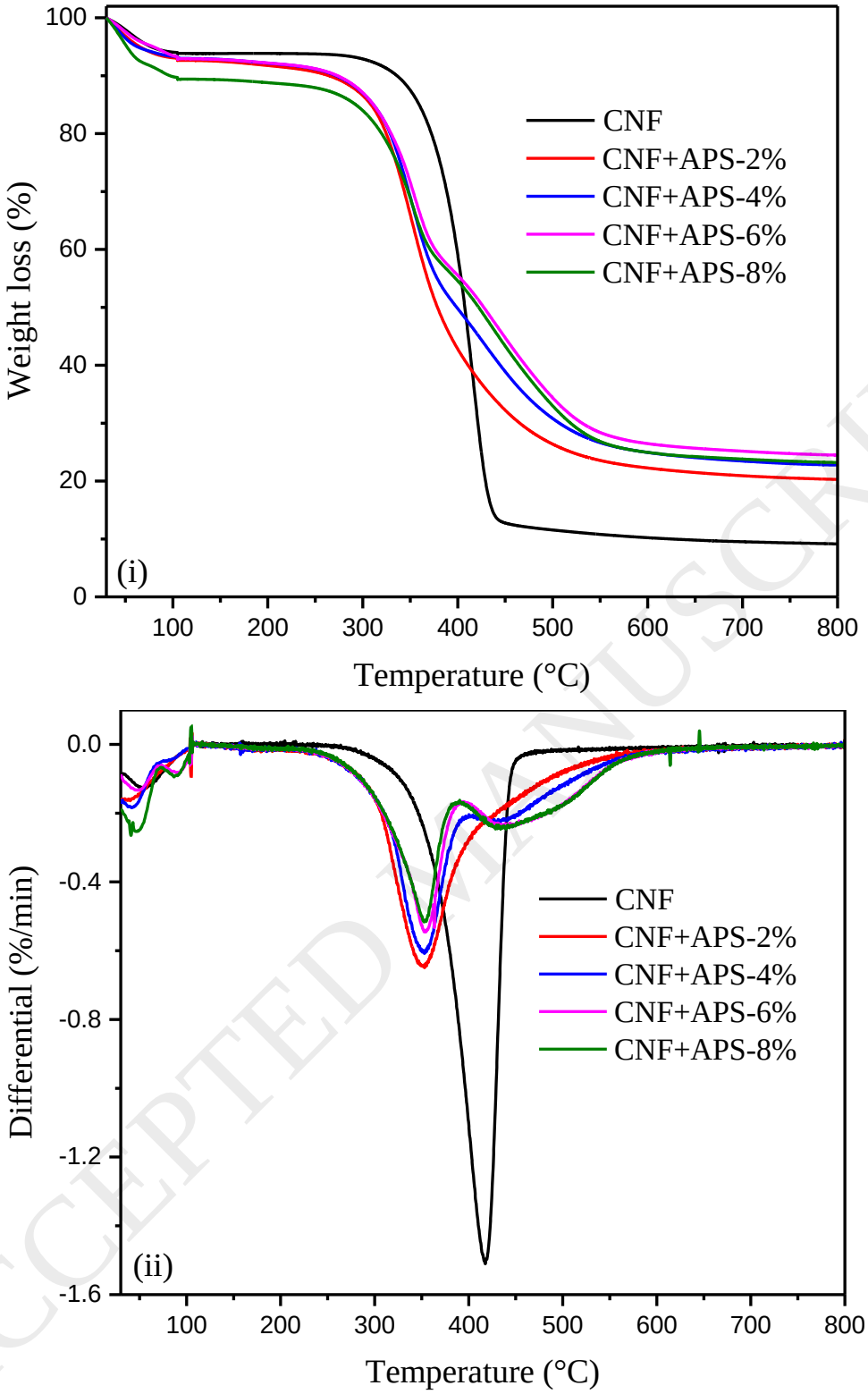

Fig. 3 TGA (i) and DTG (ii) spectra of CNF aerogels before and after modification.

3.4 XRD analysis

XRD was employed to evaluate the effect of the modification with APS on the crystalline structure of CNF before and after the modification with APS. The diffractogram of CNF before and after the modification was presented in Fig. 4. It was exhibited obvious diffraction peaks at 14.9°, 16.5°, 22.6°, and 34.5° in all samples, which corresponded to the diffraction planes of 1-10, 110, 002, and 040, respectively (Jiang, Wu, Han & Zhang, 2017). This result illustrated that the cellulose I structure (Sai et al., 2015) was intact during the modification. In addition, Fig. 4 showed that the occurrence of the broadening and weak peak at 11.8° after the modification, and their intensity was increased with the increase in the amount of added APS. This might be caused by the APS aggregates or condensate. The peak at 20.7° was assigned to amorphous phase (Jiang, Wu, Han & Zhang, 2017).

Furthermore, the crystallinity index (CrI) was calculated from formula (1) and the results are shown in Table 2. The decrease in the CrI from 70.6% to 60.3% was mainly due to the successful grafting of amorphous APS on the surface of the CNF, which increased the proportion of amorphous phase and thus reduced the total CrI. Wu et al. (Wu, Cao, Jiang & Zhang, 2017) and Mohd et al. (Mohd et al., 2016) reported the phenomenon of the reduction in crystallinity for modified cellulose. Nevertheless, the crystallite size of reflection (L_{002}) and the interlayer distance (d_{002}) of the modified CNFs did not show obvious variations after the APS modification (Table 2). This result indicated that the decrease in CrI of CNF after the modification was due to the

introduction of APS.

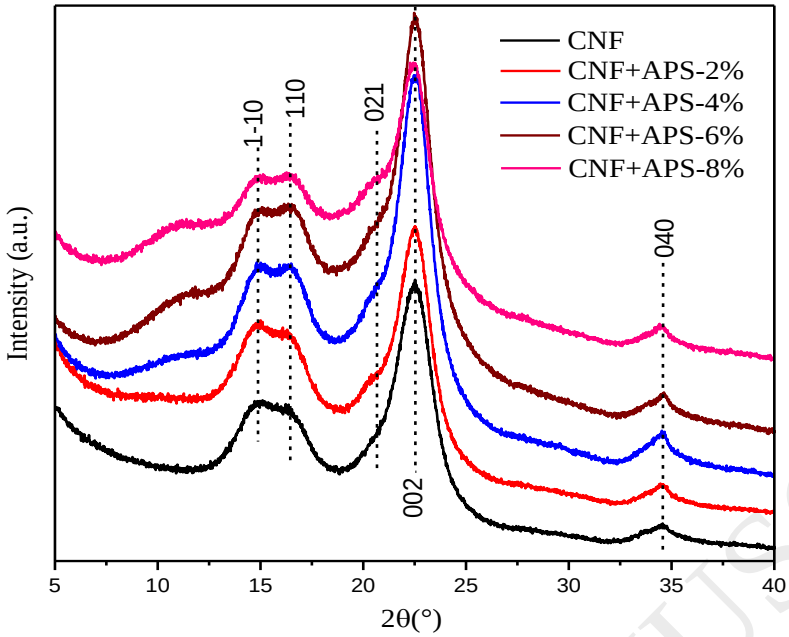

Fig. 4 XRD analysis of the CNF aerogel and the modified aerogel.

Table 2 CrI, L(002) and d(002) of CNF and the modified samples

Sample	CrI (%)	L(002)nm	d(002)nm
CNF	70.6	9.3	0.544
CNF+APS-2%	67.3	9.2	0.548
CNF+APS-4%	63.8	9.6	0.544
CNF+APS-6%	61.5	9.7	0.543
CNF+APS-8%	60.3	9.5	0.542

3.5 SEM images

SEM images of the CNF aerogel cross-section grafted with different amounts of aminosilane were presented in Fig. 5.

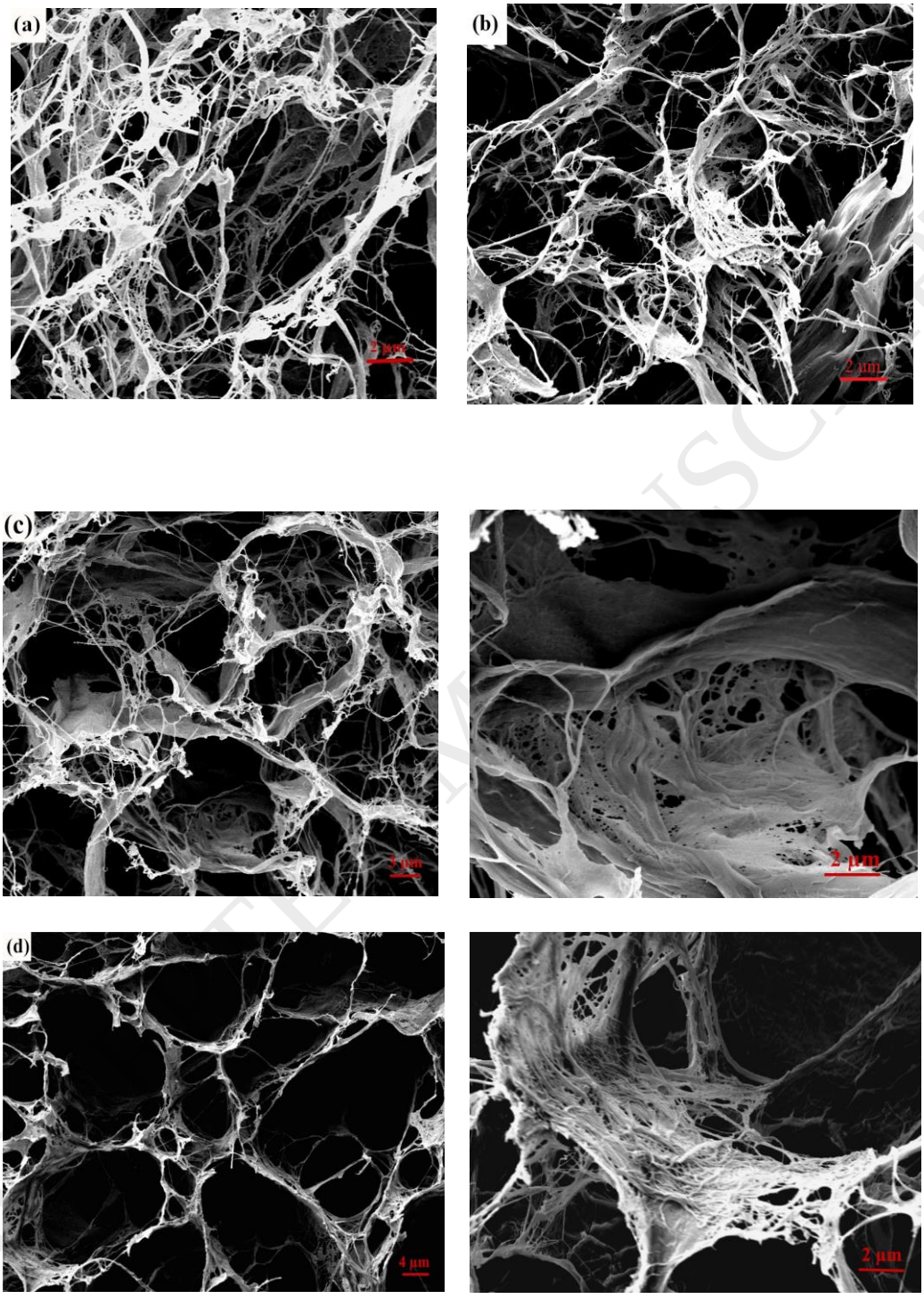

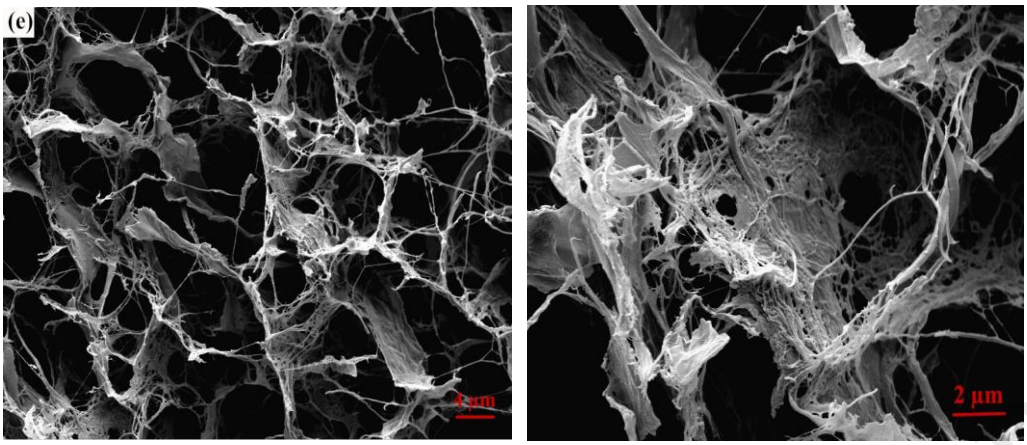

Fig. 5 SEM images of (a) CNF, (b) CNF+APS-2%, (c) CNF+APS-4%, (d) CNF+APS-6%, (e) CNF+APS-8%, the right images of (c), (d) and (e) were in higher amplification

As shown in Fig. 5, all the CNF aerogel formed a sponge-like structure after freeze-drying. The aerogel was highly porous with random pore structure and consisted of disorderly entangled nanofibrils. However, after the modification, many planar structures obviously appeared with single cellulose nanofibrils irregularly attached to the cellulose sheet (Fig. 5c, d, and e). In addition, with increase in the concentration of APS during the modification, more planar structures appeared and fewer single cellulose-nanofibrils adhered to the surface of the cellulose sheet. The plausible explanation was that the aminosilane enhanced the interaction between CNF and created more single cellulose nanofibrils form the planar structure. Moreover, it seemed that increasing the concentration of APS led to a larger average pore size of the samples (Fig. 5a-e) and showed that the surface of the aerogels became rougher, which might favored the diffusion of gas phase during the capture of CO_2 and enhanced the

adsorption capacity.

3.6 Effect of amine loading on CO_2 capture performance

Table 3. Textural properties of samples

Sample	S_{BET} (m^2/g)	V_{pore} (cm^3/g)	Average pore size (nm)	Density (kg/m^3)	Amine efficiency (mmol CO_2/mmol amine)
CNF	92.8	0.44	131.3	34.3	/
CNF+APS-2%	83.5	0.38	165.8	42.5	0.183
CNF+APS-4%	67.2	0.25	172.4	53.6	0.217
CNF+APS-6%	58.7	0.21	186.7	68.8	0.230
CNF+APS-8%	51.8	0.19	215.2	75.3	0.231

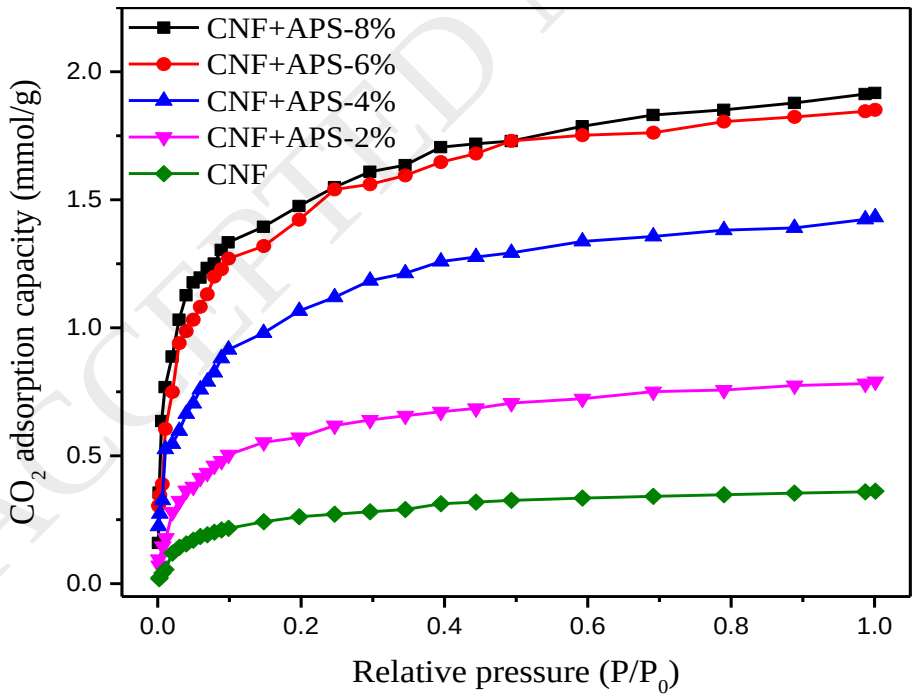

Fig. 6 CO_2 adsorption isotherms of CNF grafted with different amount APS at 1 bar with 25 ℃

The effect of amine loading on the CO_2 adsorption capacity of the CNF aerogels was investigated by measuring the CO_2 adsorption isotherms at 1 bar and 25 °C (Fig. 6). The CO_2 adsorption capacity of all samples, modified or unmodified, was dramatically enhanced with the increase in the pressure before the relative pressure of 0.1. Then, the relative pressure greater than 0.2 had insignificant effects on the CO_2 adsorption capacity. At the same time, the CO_2 adsorption capacity always increased with the increasing dose of APS. For instance, at the relative pressure of 1.0, the CO_2 adsorption capacity of the CNF aerogel was about 0.35 mmol/g. However, their capacity increased up to 0.75 and 1.91 mmol/g after the CNF was treated with 2 and 8 wt.% APS, respectively. These results illustrated that the aerogel from the amine-modified CNFs could approach the equilibrium adsorption capacity at lower partial pressure of CO_2, that the equilibrium adsorption capacity was increased with the amount of added APS during the modification. Therefore, the results indicated that the modification of CNF using APS improved significantly the CNF adsorption capacity for CO_2, and the CO_2 capacity is better than the results from Bernard et al. (1.25 mmol/g, 1 bar) (Bernard et al., 2016) and Brennan et al. (1.4 mmol/g, 1 bar) (Brennan, Thakkar, Li, Rownaghi, Koros & Rezaei, 2017) reported. In contrast, the CO_2 adsorption capacities of CNF treated with 6 and 8 wt.% APS were similar at all the pressure ranges (Fig. 6). This further supported the hypothesis that the available hydroxyl groups on the CNF surface were saturated with APS after 6 wt.% of APS was added.

It is well-known that the surface area (S_{BET}), pore volume (V_{pore}), density and efficient

nitrogen content are the four major parameters that influence the CO_2 adsorption capacity (Hao et al., 2011; Johnson, Spikowski & Schiraldi, 2009). The textural properties and the density of all samples were presented in Tab 3. It is reasonable that the CO_2 adsorption capacity and density of the modified samples increased with the increasing concentration of APS due to the higher nitrogen content contained. Meanwhile, the amine efficiency should be considered to evaluate the CO_2 capture performance, which was calculated by mmol CO_2 / mmol amine loading. High amine efficiency means the adsorbents have good CO_2 capture performance. As shown in Table 3, the high concentration of APS favored the amine efficiency, and the amine efficiency is 0.23 for the sample of CNF+APS-6%. Further increase in the APS concentration failed to increase the amine efficiency, which was in agreement with the result of elemental analysis. This result could be due to the fact the accessible hydroxyl group on the surface of CNF was saturated. Notably, the surface area and pore volume decreased after the modification of CNF aerogels (Table 3), which was also reported elsewhere (Hiyoshi, Yogo & Yashima, 2005), however the average pore size simultaneously became large which was consistent with the analysis of SEM images and favored the gas diffusion in the pore space (Drese et al., 2009; Zelenak et al., 2008).

3.7 Cyclic CO_2 capture capacity

The long-term stability of the sorbents for the cyclic CO_2 capture is one of the most important factors for practical applications and scale up (Heydari-Gorji & Sayari, 2012;

Qi, Fu, Choi & Giannelis, 2012). The regeneration process of the sorbents included the absorption of CO_2 by the polymer aerogels with outgassing at 80 °C using ASAP-20 to remove the absorbed CO_2 and any other gases.

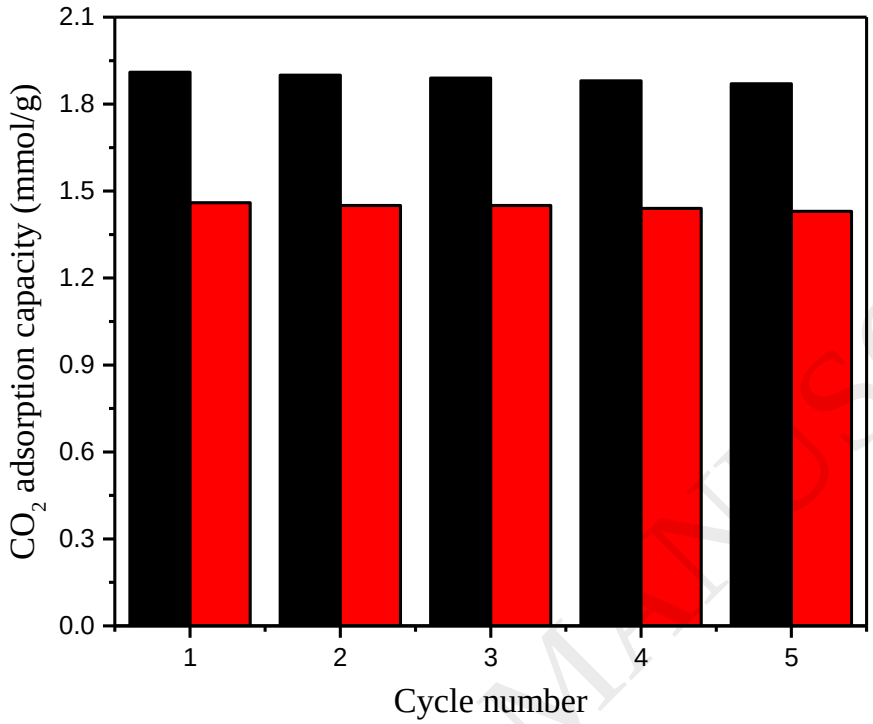

Fig. 7 Cyclic CO_2 adsorption capacity of CNF+APS-8% (black/higher) and CNF+APS-4% (red/lower).

Fig. 7 illustrated the cyclic CO_2 adsorption capacity of CNF modified with 4 and 8 wt.% APS. The adsorption capacity of CNF+APS-8% and CNF+APS-4% was 1.91 and 1.46 mmol/g for the first run, and 1.87 and 1.43 mmol/g for the fifth run, respectively. Both sorbents that were obtained lost only about 2% of the adsorption capacity of the first cycle after 5 runs. This small loss of CO_2 capacity might be ascribed to the small amount of CO_2 irreversibly chemisorbed in the polymer aerogel (Garcia-Gallastegui et al., 2012). Therefore, it was suggested that no obvious decrease in the cyclic capacity was

observed for both samples, which confirmed the structural stability of CNF after the modification. Considering the regeneration process and the cyclic CO_2 adsorption capacity, it can be assumed that the high efficient sorbents can be recycled by simply heating. These results were in agreement with the analysis of the FTIR in Fig. 2(ii).

Conclusions

In this work, amine-based hybrid aerogel adsorbents were successfully prepared via one-step chemical react with no gelation. Elemental analysis and FTIR spectra revealed that APS was successfully grafted on the surface of the CNF. Higher concentration of APS grafted on the CNF aerogels decreased slightly the thermal stability and the crystallinity of modified CNFs. However, the CO_2 adsorption capacity of the polymer aerogels were dependent on the effective amine loading on the polymer surface. The highest CO_2 adsorption capacity was 1.91 mmol/g with an amine efficiency of 0.231. Measurements of the cyclic CO_2 capacity suggested that a regeneration process could be easily achieved by heating the sample at 80 °C. These results indicated that the produced polymer aerogels for CO_2 capture might have a high prospect of use in industrial applications.

Conflicts of interest

There are no conflicts of interest to declare.

Acknowledgements

This work was financially supported by the Special Fund for Forest Scientific Research in the Public Welfare (201504603), the Priority Academic Program Development (PAPD) of Jiangsu Higher Education Institutions (China), and the USDA National Institute of Food and Agriculture, Hatch project 1012359.

References:

Aaron, D., & Tsouris, C. (2005). Separation of CO_2 from flue gas: A review. *Separation Science and Technology, 40*(1-3), 321-348.

Anuj Kumar, Y. S. N. V. (2014). Characterization of Cellulose Nanocrystals Produced by Acid-Hydrolysis from Sugarcane Bagasse as Agro-Waste. *Journal of Materials Physics and Chemistry, 2*(1), 1-8.

Aroonwilas, A., & Veawab, A. (2007). Integration of CO_2 capture unit using single- and blended-amines into supercritical coal-fired power plants: Implications for emission and energy management. *International Journal of Greenhouse Gas Control, 1*(2), 143-150.

Bacsik, Z., Atluri, R., Garcia-Bennett, A. E., & Hedin, N. (2010). Temperature-Induced Uptake of CO_2 and Formation of Carbamates in Mesocaged Silica Modified with n-Propylamines. *Langmuir, 26*(12), 10013-10024.

Bernard, F. L., Rodrigues, D. M., Polesso, B. B., Donato, A. J., Seferin, M., Chaban, V. V., Vecchia, F. D., & Einloft, S. (2016). New cellulose based ionic compounds as low-cost sorbents for CO_2 capture. *Fuel Process Technology*, 149, 131-138.

Brennan, P. J., Thakkar, H., Li, X., Rownaghi, A. A., Koros, W. J., & Rezaei, F. (2017). Effect of Post-Functionalization Conditions on the Carbon Dioxide Adsorption Properties of Aminosilane-Grafted Zirconia/Titania/Silica-Poly(amide-imide) Composite Hollow Fiber Sorbents. *Energy Technology, 5*(2), 327-337.

Cheng, Q., Wang, S., Rials, T. G., & Lee, S. (2007). Physical and mechanical properties of polyvinyl alcohol and polypropylene composite materials reinforced with fibril aggregates isolated from regenerated cellulose fibers. *Cellulose, 14*(6), 593-602.

Choi, S., Drese, J. H., & Jones, C. W. (2009). Adsorbent Materials for Carbon Dioxide Capture from Large Anthropogenic Point Sources. *ChemSusChem, 2*(9), 796-854.

Danon, A., Stair, P. C., & Weitz, E. (2011). FTIR Study of CO_2 Adsorption on Amine-Grafted SBA-15: Elucidation of Adsorbed Species. *Journal of Physical Chemistry C, 115*(23), 11540-11549.

Drese, J. H., Choi, S., Lively, R. P., Koros, W. J., Fauth, D. J., Gray, M. L., & Jones, C. W. (2009). Synthesis-Structure-Property Relationships for Hyperbranched Aminosilica CO_2 Adsorbents. *Advanced Functional Materials, 19*(23), 3821-3832.

Garcia-Gallastegui, A., Iruretagoyena, D., Gouvea, V., Mokhtar, M., Asiri, A. M., Basahel, S. N., Al-Thabaiti, S. A., Alyoubi, A. O., Chadwick, D., & Shaffer, M. S. P. (2012). Graphene Oxide as Support for Layered Double Hydroxides: Enhancing the CO_2 Adsorption Capacity. *Chemistry of Materials,*

24(23), 4531-4539.

Garvey, C. J., Parker, I. H., & Simon, G. P. (2005). On the interpretation of X-ray diffraction powder patterns in terms of the nanostructure of cellulose I fibres. *Macromolecular Chemistry and Physics, 206*(15), 1568-1575.

Gavillon, R., & Budtova, T. (2008). Aerocellulose: new highly porous cellulose prepared from cellulose-NaOH aqueous solutions. *Biomacromolecules, 9*(1), 269-277.

Gebald, C., Wurzbacher, J. A., Tingaut, P., Zimmermann, T., & Steinfeld, A. (2011). Amine-Based Nanofibrillated Cellulose As Adsorbent for CO_2 Capture from Air. *Environmental Science & Technology, 45*(20), 9101-9108.

Habibi, Y., Lucia, L. A., & Rojas, O. J. (2010). Cellulose nanocrystals: chemistry, self-assembly, and applications. *Chemical Reviews, 110*(6), 3479-3500.

Hao, G., Li, W., Qian, D., Wang, G., Zhang, W., Zhang, T., Wang, A., Schueth, F., Bongard, H., & Lu, A. (2011). Structurally Designed Synthesis of Mechanically Stable Poly(benzoxazine-co-resol)-Based Porous Carbon Monoliths and Their Application as High-Performance CO_2 Capture Sorbents. *Journal of The American Chemical Society, 133*(29), 11378-11388.

Haszeldine, R. S. (2009). Carbon Capture and Storage: How Green Can Black Be? *Science, 325*(5948), 1647-1652.

Heydari-Gorji, A., & Sayari, A. (2012). Thermal, Oxidative, and CO_2-Induced Degradation of Supported Polyethylenimine Adsorbents. *Industrial & Engineering Chemistry Research, 51*(19), 6887-6894.

Hiyoshi, N., Yogo, K., & Yashima, T. (2005). Adsorption characteristics of carbon dioxide on organically

functionalized SBA-15. *Microporous & Mesoporous Materials*.

Hokkanen, S., Repo, E., Suopajarvi, T., Liimatainen, H., Niinimaa, J., & Sillanpaa, M. (2014). Adsorption of Ni(II), Cu(II) and Cd(II) from aqueous solutions by amino modified nanostructured microfibrillated cellulose. *Cellulose, 21*(3), 1471-1487.

Hosseinaei, O., Wang, S., Enayati, A. A., & Rials, T. G. (2012). Effects of hemicellulose extraction on properties of wood flour and wood-plastic composites. *Composites Part Applied Science and Manufacturing, 43*(4), 686-694.

Hosseinaei, O., Wang, S., Taylor, A. M., & Kim, J. (2012). Effect of hemicellulose extraction on water absorption and mold susceptibility of wood-plastic composites. *International Biodeterioration & Biodegradation, 71*, 29-35.

Jiang, H., Wu, Y., Han, B., & Zhang, Y. (2017). Effect of oxidation time on the properties of cellulose nanocrystals from hybrid poplar residues using the ammonium persulfate. *Carbohydrate Polymers, 174*, 291-298.

Jiao, J., Cao, J., Xia, Y., & Zhao, L. (2016). Improvement of adsorbent materials for CO_2 capture by amine functionalized mesoporous silica with worm-hole framework structure. *Chemical Engineering Journal, 306*, 9-16.

Johnson, J. R. I., Spikowski, J., & Schiraldi, D. A. (2009). Mineralization of Clay/Polymer Aerogels: A Bioinspired Approach to Composite Reinforcement. *ACS Applied Materials & Interfaces, 1*(6), 1305-1309.

Jones, C. W. (2011). CO_2 Capture from Dilute Gases as a Component of Modern Global Carbon

Management. In J. M. Prausnitz. *Annual Review of Chemical and Biomolecular Engineering* pp. 31-52).

Kalia, S., Boufi, S., Celli, A., & Kango, S. (2014). Nanofibrillated cellulose: surface modification and potential applications. *Colloid and Polymer Science, 292*(1), 5-31.

Knoefel, C., Martin, C., Hornebecq, V., & Llewellyn, P. L. (2009b). Study of Carbon Dioxide Adsorption on Mesoporous Aminopropylsilane-Functionalized Silica and Titania Combining Microcalorimetry and in Situ Infrared Spectroscopy. *Journal of Physical Chemistry C, 113*(52), 21726-21734.

L. Segal, J. C. A. M. (1959). An empirical method for estimating the degree of crystallinity of native cellulose using the x-ray diffractometer. *Textile Research Journal, 29*(10), 786-794.

Lee, K., Quero, F., Blaker, J. J., Hill, C. A. S., Eichhorn, S. J., & Bismarck, A. (2011). Surface only modification of bacterial cellulose nanofibres with organic acids. *Cellulose, 18*(3), 595-605.

Linsha, V., Mohamed, A. P., & Ananthakumar, S. (2015). Nanoassembling of thixotropically reversible alumino-siloxane hybrid gels to hierarchically porous aerogel framework. *Chemical Engineering Journal, 259*, 313-322.

Lu, J., Askeland, P., & Drzal, L. T. (2008). Surface modification of microfibrillated cellulose for epoxy composite applications. *Polymer, 49*(5), 1285-1296.

Meng, Y., Young, T. M., Liu, P., Contescu, C. I., Huang, B., & Wang, S. (2015). Ultralight carbon aerogel from nanocellulose as a highly selective oil absorption material. *Cellulose, 22*(1), 435-447.

Mohd, N. H., Ismail, N. F. H., Zahari, J. I., Fathilah, W. F. B. W., Kargarzadeh, H., Ramli, S., Ahmad, I., Yarmo, M. A., & Othaman, R. (2016). Effect of Aminosilane Modification on Nanocrystalline Cellulose Propertiesq. *Journal of Nanomaterials* (4804271).

Nguyen, S. T., Feng, J., Ng, S. K., Wong, J. P. W., Tan, V. B. C., & Duong, H. M. (2014). Advanced thermal insulation and absorption properties of recycled cellulose aerogels. *Colloids and Surfaces A-Physicochemical and Engineering Aspects, 445*, 128-134.

Pacheco, D. M., Johnson, J. R., & Koros, W. J. (2012). Aminosilane-Functionalized Cellulosic Polymer for Increased Carbon Dioxide Sorption. *Industrial & Engineering Chemistry Research, 51*(1), 503-514.

Popescu, C., Singurel, G., Popescu, M., Vasile, C., Argyropoulos, D. S., & Willfor, S. (2009). Vibrational spectroscopy and X-ray diffraction methods to establish the differences between hardwood and softwood. *Carbohydrate Polymers, 77*(4), 851-857.

Primo, A., Forneli, A., Corma, A., & Garcia, H. (2012). From Biomass Wastes to Highly Efficient CO_2 Adsorbents: Graphitisation of Chitosan and Alginate Biopolymers. *ChemSusChem, 5*(11), 2207-2214.

Qi, G., Fu, L., Choi, B. H., & Giannelis, E. P. (2012). Efficient CO_2 sorbents based on silica foam with ultra-large mesopores. *Energy & Environmental Science, 5*(6), 7368-7375.

Robinson, K., McCluskey, A., & Attalla, M. I. (2011). An FTIR Spectroscopic Study on the Effect of Molecular Structural Variations on the CO_2 Absorption Characteristics of Heterocyclic Amines. *ChemPhysChem, 12*(6), 1088-1099.

Rownaghi, A. A., Kant, A., Li, X., Thakkar, H., Hajari, A., He, Y., Brennan, P. J., Hosseini, H., Koros, W. J., & Rezaei, F. (2016). Aminosilane-Grafted Zirconia-Titiania-Silica Nanoparticles/Torlon Hollow Fiber Composites for CO_2 Capture. *ChemSusChem, 9*(10), 1166-1177.

Sai, H., Fu, R., Xing, L., Xiang, J., Li, Z., Li, F., & Zhang, T. (2015). Surface Modification of Bacterial Cellulose Aerogels' Web-like Skeleton for Oil/Water Separation. *ACS Applied Materials & Interfaces,*

7(13), 7373-7381.

Sangchoom, W., & Mokaya, R. (2015). Valorization of Lignin Waste: Carbons from Hydrothermal Carbonization of Renewable Lignin as Superior Sorbents for CO_2 and Hydrogen Storage. *ACS Sustainable Chemistry & Engineering, 3*(7), 1658-1667.

Sevilla, M., & Fuertes, A. B. (2011). Sustainable porous carbons with a superior performance for CO_2 capture. *Energy & Environmental Science, 4*(5), 1765-1771.

She, Y., Zhang, H., Song, S., Lang, Q., & Pu, J. (2013). Preparation and Characterization of Waterborne Polyurethane Modified by Nanocrystalline Cellulose. *BioResources, 8*(2), 2594-2604.

Sumida, K., Rogow, D. L., Mason, J. A., McDonald, T. M., Bloch, E. D., Herm, Z. R., Bae, T., & Long, J. R. (2012). Carbon Dioxide Capture in Metal-Organic Frameworks. *Chemical Reviews, 112*(2SI), 724-781.

Versteeg, G. F., Van Dijck, L., & Van Swaaij, W. (1996). On the kinetics between CO_2 and alkanolamines both in aqueous and non-aqueous solutions. An overview. *Chemical Engineering Communication, 144*, 113-158.

Wu, Y., Cao, F., Jiang, H., & Zhang, Y. (2017). Preparation and characterization of aminosilane-functionalized cellulose nanocrystal aerogel. *Materials Research Express, 4*(0853038).

Yu, K. M. K., Curcic, I., Gabriel, J., & Tsang, S. C. E. (2008). Recent Advances in CO_2 Capture and Utilization. *ChemSusChem, 1*(11), 893-899.

Zelenak, V., Badanicova, M., Halamova, D., Cejka, J., Zukal, A., Murafa, N., & Goerigk, G. (2008). Amine-modified ordered mesoporous silica: Effect of pore size on carbon dioxide capture. *Chemical*

Engineering Journal, *144*(2), 336-342.

Zhai, T., Zheng, Q., Cai, Z., Xia, H., & Gong, S. (2016). Synthesis of polyvinyl alcohol/cellulose nanofibril hybrid aerogel microspheres and their use as oil/solvent superabsorbents. *Carbohydrate Polymers*, *148*, 300-308.

Zhang, Z., Sebe, G., Rentsch, D., Zimmermann, T., & Tingaut, P. (2014). Ultralightweight and Flexible Silylated Nanocellulose Sponges for the Selective Removal of Oil from Water. *Chemistry of Materials, 26*(8), 2659-2668.

Zu, G., Shen, J., Wang, W., Zou, L., Lian, Y., & Zhang, Z. (2015). Silica-Titania Composite Aerogel Photocatalysts by Chemical Liquid Deposition of Titania onto Nanoporous Silica Scaffolds. *ACS Applied Materials & Interfaces*, *7*(9), 5400-5409.